



Phase Transitions

A Multinational Journal

ISSN: 0141-1594 (Print) 1029-0338 (Online) Journal homepage: <https://www.tandfonline.com/loi/gpht20>

On the possible internal structure of the ferroelectric Ising lines in BaTiO₃

V. Stepkova & J. Hlinka

To cite this article: V. Stepkova & J. Hlinka (2017) On the possible internal structure of the ferroelectric Ising lines in BaTiO₃, Phase Transitions, 90:1, 11-16, DOI: [10.1080/01411594.2016.1206543](https://doi.org/10.1080/01411594.2016.1206543)

To link to this article: <https://doi.org/10.1080/01411594.2016.1206543>



© 2016 The Author(s). Published by Informa UK Limited, trading as Taylor & Francis Group



Published online: 26 Jul 2016.



Submit your article to this journal [↗](#)



Article views: 448



View related articles [↗](#)




View Crossmark data [↗](#)



Citing articles: 3 View citing articles [↗](#)

On the possible internal structure of the ferroelectric Ising lines in BaTiO₃

V. Stepkova and J. Hlinka 

Institute of Physics, The Czech Academy of Sciences, Praha, Czech Republic

ABSTRACT

This article is devoted to a detailed analysis of the inner structure of the Ising line, a topological defect separating two parts of a ferroelectric Bloch domain wall with opposite helicity, in the framework of the phenomenological Ginzburg–Landau–Devonshire model. Results performed for Ising lines in a $\langle 211 \rangle$ -oriented 180-degree domain wall of rhombohedral BaTiO₃ suggest remarkably strong dependence of the polarization profiles on the form of gradient terms. Profiles of the skyrmion density, vorticity and divergence of the polarization field were calculated numerically in the few-nm vicinity of the Ising line defect.

ARTICLE HISTORY

Received 8 April 2016
Accepted 20 June 2016

KEYWORDS

Ginzburg–Landau–Devonshire model; phase-field; BaTiO₃; topological defects

1. Introduction

Topological defects play an important role in many areas of physics, ranging from particle physics to cosmology and liquid crystals science. Domain boundaries belong to the standard examples of such defects in the field of ferroelectric and ferromagnetic materials.[1] Over the last few years, however, more and more attention is paid to lower dimensional topological defects in these materials, such as skyrmion lines, vortex cores, domain-wall junctions or intersections, point like hedgehog defects, etc. [2–6].

Recently, we have performed phase-field simulations of an interesting object of this type – a line defect forming a border between two parts of a ferroelectric Bloch domain wall, associated with opposite signs of helicity.[7] The calculations were performed in the framework of the phenomenological Ginzburg–Landau–Devonshire (GLD) model, assuming $\langle 211 \rangle$ -oriented 180-degree domain wall in the rhombohedral phase of BaTiO₃. Considering an ideal dielectric material described by the standard set of the coefficients of the Landau energy profiles, the polarization gradient terms and the lowest-order elastic, electrostrictive and electrostatic interactions in the rhombohedral BaTiO₃, it was possible to estimate that such defect has a form of about 2 nm diameter nanorod with an unpolarized core. Since the polarization is vanishing in its core, it has been denoted as an Ising line.

These Ising lines are likely to be highly mobile objects, because the 2 nm diameter is sufficiently large in comparison with the interatomic distances to make the crystal lattice pinning ineffective. This was actually one of the main obstacles in previous phase-field investigations. The adopted phenomenological model provides only a crude approximation to the real material and uncertainties in the parameter values imply that predictions are only semi-quantitative results. Nevertheless, basic properties of Ising lines reported in [7] are robust results, dictated by the dominating in energy electrostatic interactions.

The purpose of this paper is to explore in more details the 2–3 nm diameter core of the Ising line, i.e. the region which can be characterized by topologically protected local anomalies of the differential quantities like the skyrmion density,[8] vorticity [9] but also the simple divergence. At the same time, we would like to demonstrate that the geometry of the inner structure of the core of the Ising line is rather strongly sensitive to the values and to the anisotropy of the polarization gradient energy term.

2. Bloch walls and Ising lines for different gradient terms

The skyrmion density, vorticity and divergence of the polarization field around the Ising line shown in this paper were determined for the same model,[10,11] the same parameters [7] and in the same overall geometry, shown schematically in Figure 1, as previously.[7] The simulation box size was $256 \times 256 \times 256$ or $128 \times 256 \times 256$ sites. The simulation was performed at $T = 118$ K under stress-free periodic boundary conditions, spatial discretization step was fixed to 0.25 nm and time step to 2 fs, and the computer simulation was done using phase-field approach of Ref. [12].

The alternating thick layers shown in Figure 1 are domains with polarization along $[111]$ and $[\bar{1}\bar{1}\bar{1}]$ directions, the intermediate thin layers stand for 180-degree Bloch domain boundaries divided into regions with opposite helicities and opposite components of the internal polarization, oriented along $[0\bar{1}1]$ and $[01\bar{1}]$ crystallographic directions. Let us note that these special directions are related to the electric and elastic compatibility conditions on the domain walls and Ising lines, and for the sake of coherence with the previous work,[10] they are associated with auxiliary, symmetry-adapted Cartesian coordinate system $\{r, s, t\}$, also indicated in Figure 1.

From the symmetry point of view, the domain structure is associated with macroscopic symmetry breaking from $m\bar{3}m$ to $3m$ point group (species #186 of Ref.[13]). The Ising wall with $s \parallel [\bar{2}11]$ direction would have $2/m$ symmetry (with $2 \parallel \mathbf{t}$), while the symmetry of the Bloch wall reduces to 2. Finally, the Ising line as an individual object has merely the inversion symmetry. Overall symmetry lowering implies that the Ising line may occur in 24 equivalent orientational states ($m\bar{3}m > \bar{1}$, species #211 of Ref. [13]).

The formation of the equidistant parallel 180-degree walls with $[\bar{2}11]$ orientation was facilitated by the choice of the initial and periodic boundary conditions, but the structure was than fully relaxed, so that the resulting polarization profiles, the orientation of the Ising lines, etc. can be viewed as a numerically found stationary solution of three-dimensional (3D) integro-differential Euler–Lagrange equations of the GLD model under the prescribed periodic boundary conditions. Moreover, the stability of the structure under small perturbations was tested.[7] Obviously, sufficiently large external electric field eventually switch the structure to the monodomain state.[7]

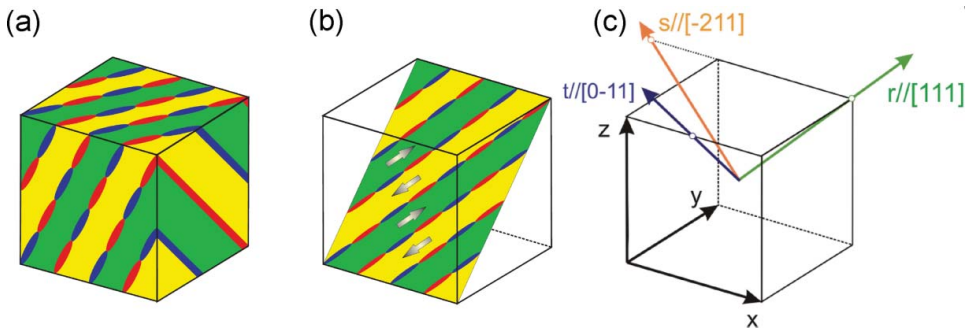


Figure 1. (a) Schematic illustration of simulated domain structure having Ising lines within 180-degree chiral domain walls. Alternating lamellae correspond to $[111]$ and $[\bar{1}\bar{1}\bar{1}]$ domain states, respectively. Each domain wall is composed of alternating stripes of opposite polarization, corresponding to Bloch wall regions with opposite helicities. (b) The polarization distribution within $(0\bar{1}1)$ plane perpendicular to domain wall (P_z) polarization component. (c) Symmetry-adapted Cartesian coordinate system.

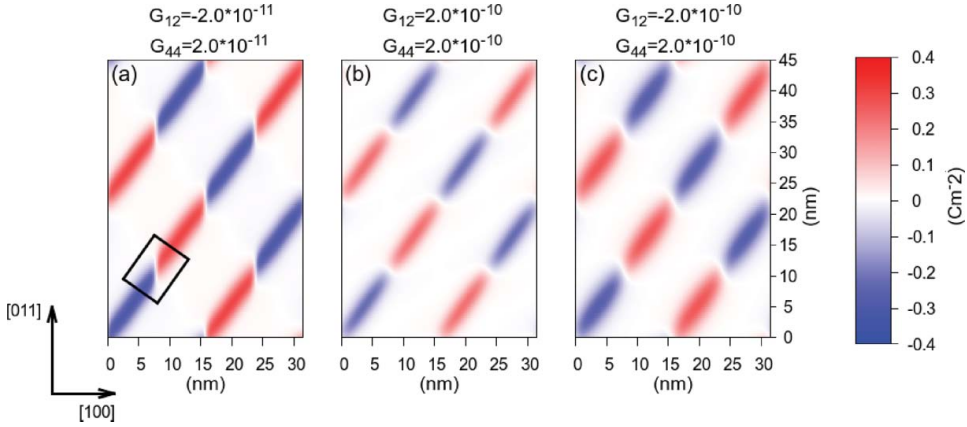


Figure 2. P_t polarization component distribution obtained for different gradient parameters within $(0\bar{1}1)$ plane shown in Figure 1 (b).

Resulting polarization pattern is independent on the coordinate \mathbf{t} , and, therefore, it is useful to inspect the distribution of the polarization within this $(0\bar{1}1)$ plane only. In Figure 2, we only show the distribution of the P_t component. The thick stripes with zero values of P_t correspond to the bulk ferroelectric domains. The areas of nonzero P_t are concentrated in narrow stripes, representing sections of the plane by ferroelectric Bloch walls. The sectors with positive or negative P_t are shaded. Tiny unpolarized areas with ($P_t \approx 0$) in between these sectors are the locations of the Ising lines.

Figure 2(a) is showing the distribution of P_t component calculated with the standard model parameters.[10,11] In comparison, the same calculation is performed with slightly modified values of the gradient term of the GLD functional, $\frac{1}{2} G_{ijkl} \frac{\partial P_i}{\partial x_j} \frac{\partial P_k}{\partial x_l}$. The gradient coefficients [10] values are marked in the figure. It is clear that the profile of the P_t component is strongly influenced in the core area of the Ising line. In particular, the Bloch walls in Figure 2(a) are interrupted roughly along the lines parallel to the $[011]$ direction, while the Bloch wall in Figure 2(b) are interrupted roughly along the lines perpendicular to the direction of the wall.

Although the profile of the P_t component around the Ising line is strongly sensitive to the gradient term coefficients, we are not aware of any experimental or theoretical results that would allow us to appreciate which of the profiles shown in Figure 2 is more similar to the real Ising-line core structure. As far as we know, the only recent attempt to refine the gradient term was undertaken in Ref. [14]. Therefore, in the following, we shall rely on the values used in Figure 2(a), estimated originally in Ref.[11] from inelastic neutron scattering data on soft phonon branch dispersion and used systematically in a set of subsequent studies.[15–20]

3. Skyrmion density, vorticity and divergence

In order to evaluate the spatial derivatives involved in differential quantities, such as in the skyrmion density, vorticity and divergence, we have simulated the 3D vectorial profile of the polarization on a dense mesh with 0.25 nm steps in all cartesian coordinates and then smoothly interpolated the simulated profile by convenient analytic functions. The smoothed profile of the polarization around the Ising line, denoted by rectangular in Figure 2(a), is shown in Figure 3. The profile can be viewed as the numerically calculated profile of the Ising line in the continuous limit.

Partial derivatives of this polarization profile allow to evaluate the vorticity field $\nabla \times \mathbf{P}$ and the divergence field $\nabla \cdot \mathbf{P}$, all shown in Figure 4. As expected, $\nabla \cdot \mathbf{P}$, related to uncompensated residual charge, is rather small, while the vorticity is quite pronounced, capturing the curl nature of the Ising

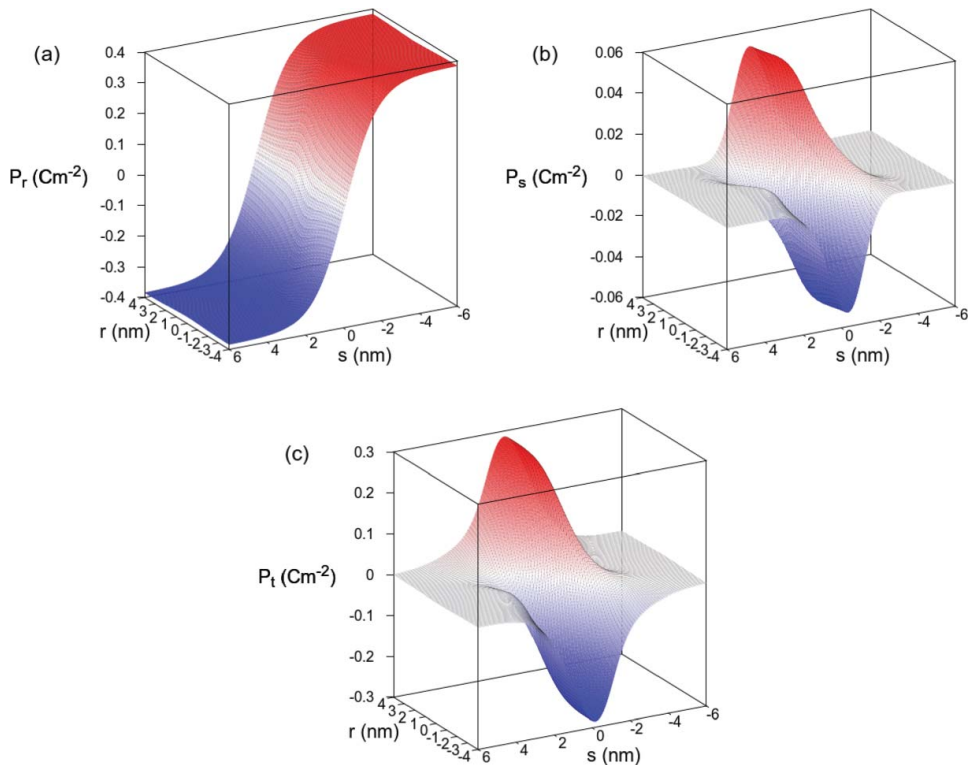


Figure 3. Profiles of the polarization components in the vicinity of the Ising line.

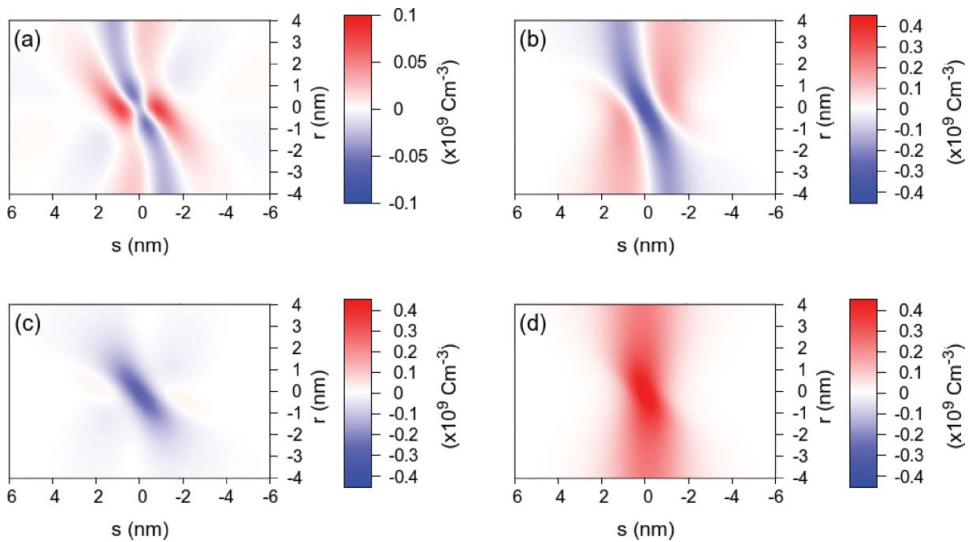


Figure 4. (a) Divergence field $(\nabla \cdot \mathbf{P})$ and the components of vorticity field (b) $(\nabla \times \mathbf{P})_r$, (c) $(\nabla \times \mathbf{P})_s$, (d) $(\nabla \times \mathbf{P})_t$ in the vicinity of the Ising line, indicated in Figure 2(a).

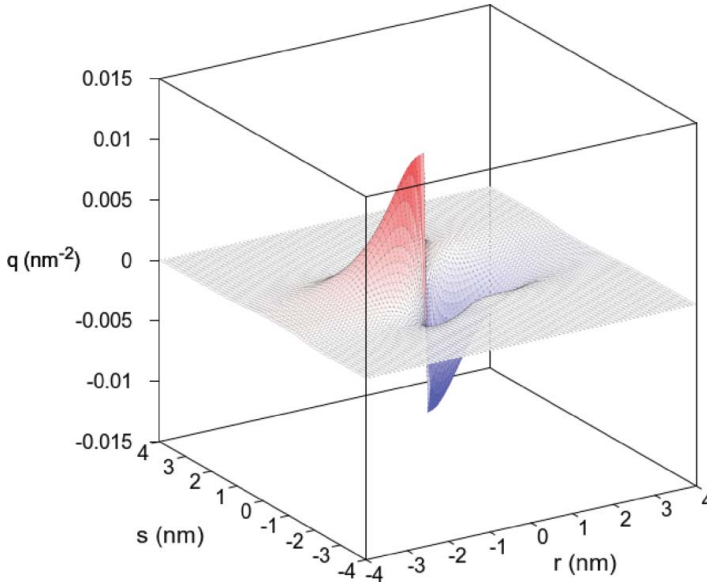


Figure 5. Skyrmion density in the vicinity of the Ising line has a form of skyrmionic dipole.

line. For the sake of completeness, we have also evaluated the skyrmion density [8]

$$q = \frac{1}{4\pi} \frac{\mathbf{P}}{|\mathbf{P}|} \cdot \left(\partial_r \frac{\mathbf{P}}{|\mathbf{P}|} \times \partial_s \frac{\mathbf{P}}{|\mathbf{P}|} \right), \quad (1)$$

which measures solid angle covered by the outgoing polarization directions around the defect. As could be expected from Ising-line symmetry, the overall integral of the skyrmion density is zero, and even if considered as skyrmionic dipole (see Figure 5), its value is rather small. Due to the obvious electrostatic reasons, the polarization directions around the defect are avoiding polarization pointing along the s direction.

Finally, let us note that the helicity Q of a ferroelectric Bloch wall can be formally defined in a close analogy to the magnetic Bloch wall [21] as

$$Q = \frac{1}{\pi |\mathbf{P}|^2} \int_{-\infty}^{\infty} \mathbf{P} \cdot \frac{\partial \mathbf{P}}{\partial s} ds. \quad (2)$$

However, for the obvious symmetry reasons, right at the Ising line, this integral is zero.

4. Conclusions

In conclusion, the present analysis gives insight in an inner structure of the interesting topological defect, predicted to exist within ferroelectric Bloch walls of rhombohedral BaTiO_3 . We have shown how strongly it depends on the coefficients of the gradient term. This finding suggests that knowledge of the detailed atomistic structure around such defect, for example from a future ab-initio calculation, could bring a very stringent test for the gradient term values. We have also calculated the profile of the polarization components and related differential quantities.

Acknowledgements

Authors thank their colleague Pavel Márton for fruitful discussions and continuous development of the ferodo software package.


Disclosure statement

No potential conflict of interest was reported by the authors.

Funding

This work was supported by the Czech Science Foundation [grant number 15-04121S].

ORCID

J. Hlinka  <http://orcid.org/0000-0002-9293-4462>

References

- [1] Mermin ND. The topological theory of defects in ordered media. *Rev Mod Phys.* **1979**;51:591–648.
- [2] Seidel J, editor. Topological structures in ferroic materials. Cham: Springer International Publishing; **2016**.
- [3] Ivry Y, Chu DP, Scott JF, et al. Flux closure vortex like domain structures in ferroelectric thin films. *Phys Rev Lett.* **2010**;104:207602.
- [4] Gregg JM. Exotic domain states in ferroelectrics: searching for vortices and skyrmions. *Ferroelectrics.* **2012**;433:74–87.
- [5] Chang LW, Nagarajan V, Scott JF, et al. Self-similar nested flux closure structures in a tetragonal ferroelectric. *Nano Lett.* **2013**;13:2553–2557.
- [6] Prosandeev S, Ponomareva I, Naumov I, et al. Original properties of dipole vortices in zero-dimensional ferroelectrics. *J Phys Condens. Matter.* **2008**;20:193201.
- [7] Stepkova V, Marton P, Hlinka J. Ising lines: natural topological defects within ferroelectric Bloch walls. *Phys Rev B.* **2015**;92:094106.
- [8] Nahas Y, Prokhorenko S, Louis L, et al. Discovery of stable skyrmionic state in ferroelectric nanocomposites. *Nat Commun.* **2015**;6:8542.
- [9] Yadav AK, Nelson CT, Hsu SL, et al. Observation of polar vortices in oxide superlattices. *Nature.* **2016**;530:198–201.
- [10] Marton P, Rychetsky I, Hlinka J. Domain walls of ferroelectric BaTiO₃ within Ginzburg-Landau-Devonshire phenomenological model. *Phys Rev B.* **2010**;81:144125.
- [11] Hlinka J, Marton P. Phenomenological model of a 90° domain wall in BaTiO₃-type ferroelectrics. *Phys Rev B.* **2006**;74:104104.
- [12] Marton P, Hlinka J. Simulation of domain patterns in BaTiO₃. *Phase Transitions* **2006**;79:467–483.
- [13] Hlinka J, Privratska J, Ondrejovic P, et al. Symmetry guide to ferroaxial transitions. *Phys Rev Lett.* **2016**;116:177602.
- [14] Taherinejad M, Vanderbilt D, Marton P, et al. Bloch-type domain walls in rhombohedral BaTiO₃. *Phys Rev B.* **2012**;86:155138.
- [15] Hlinka J, Ondrejovic P, Marton P. The piezoelectric response of nanotwinned BaTiO₃. *Nanotechnology.* **2009**;20:105709.
- [16] Hlinka J, Stepkova V, Marton P, et al. Phase-field modelling of 180° "Bloch walls" in rhombohedral BaTiO₃. *Phase Transit.* **2011**;84:738–746.
- [17] Stepkova V, Marton P, Hlinka J. Stress-induced phase transition in ferroelectric domain walls of BaTiO₃. *J Phys Condens Matter.* **2012**;24:212201.
- [18] Marton P, Stepkova V, Hlinka J. Divergence of dielectric permittivity near phase transition within ferroelectric domain boundaries. *Phase Transit.* **2013**;86:103–108.
- [19] Stepkova V, Marton P, Setter N, et al. Closed-circuit domain quadruplets in BaTiO₃ nanorods embedded in SrTiO₃ film. *Phys Rev B.* **2014**;89:060101(R).
- [20] Hlinka J, Stepkova V, Marton P, et al. Ferroelectric domain walls and their intersections in phase-field simulations. In: Seidel J, editor. Topological structures in ferroic materials. Cham: Springer International Publishing; **2016**. p. 161–180.
- [21] Baryakhtar V, Krotchenko E, Yablonsky D. Magnetic symmetry of domain walls with Bloch lines in ferromagnets and ferrites. *Sov Phys JETP.* **1986**;64:542–548.